Generation of broadband terahertz radiation using a backward wave oscillator and pseudospark-sourced electron beam

W. He, L. Zhang, D. Bowes, H. Yin, K. Ronald, A. D. R. Phelps, and A. W. Cross
Department of Physics, SUPA, University of Strathclyde, Glasgow, G4 0NG Scotland, United Kingdom

(Received 29 July 2015; accepted 20 September 2015; published online 28 September 2015)

This paper presents for the generation of a small size high current density pseudospark (PS) electron beam for a high frequency (0.2 THz) Backward Wave Oscillator (BWO) through a Doppler up-shift of the plasma frequency. An electron beam ~1 mm diameter carrying a current of up to 10 A and current density of 10^8 A m^{-2}, with a sweeping voltage of 42 to 25 kV and pulse duration of 25 ns, was generated from the PS discharge. This beam propagated through the rippled-wall slow wave structure of a BWO beam-wave interaction region in a plasma environment without the need for a guiding magnetic field. Plasma wave assisted beam-wave interaction resulted in broadband output over a frequency range of 186–202 GHz with a maximum power of 20 W. [http://dx.doi.org/10.1063/1.4932099]

Generation of terahertz radiation ranging in the frequency band from 100 GHz to 3 THz is a recognized technological gap, where conventional optical and electronic technologies are struggling to provide good frequency bandwidth at even rather moderate power levels. Addressing this power-bandwidth deficit in the low THz range a table-top Backward Wave Oscillator (BWO) based on a pseudospark (PS) electron beam was studied. BWOs,[1] like Free Electron Lasers[2] and gyro-BWOs,[3,4] are tunable but the main advantages of a pseudospark driven BWO over these similar devices are portability and low cost due to not having to use either a high magnetic field or a large accelerator facility. The pseudospark-based electron device does not require the use of a guide magnetic field therefore it opens up the possibility of inexpensive, powerful hand-held THz radiation sources. Moreover, the PS discharge can be initialized by a pulsed voltage;[5] therefore, the whole device including the voltage source could be fitted in a hand-held volume and weight and operated in a torch-like fashion. A PS discharge can typically achieve a pulse repetition rate of a few thousand hertz.[6] Because of its high current emission, special discharge characteristics, long lifetime,[7] and hence, a diverse range of potential applications, the low temperature PS discharge[8,9] has gained great attention during the last 30 years.

In a BWO, the beam and its associated growing plasma oscillations propagate in the opposite direction to the growth of the electromagnetic wave, with the beam modulation amplitude greatest at the downstream end of the slow wave structure (SWS) while the wave amplitude is greatest at the upstream end. A wide frequency tuning bandwidth can be achieved by adjusting the electron beam voltage to alter the synchronous frequency.

To achieve higher BWO output power levels in the THz range, a higher current density electron beam is required, preferably of the order of 10^6 A m^{-2}. In satisfying the beam requirements for THz devices, the pseudospark-sourced electron beam has appeared to be very attractive, with the highest combined beam current density ($>10^8$ A m^{-2}) and brightness (up to 10^{12} A m^{-2} rad^{-2}).[10,11]

The experimental configuration is shown in Fig. 1. The discharge chamber in the PS discharge system consisted of a planar anode and a planar cathode with a cylindrical hollow cavity, between which were placed three intermediate electrodes of 3 mm thickness and four Perspex insulation discs of 4 mm thickness. The anode and cathode and electrodes were made of stainless steel and have an on-axis hole of 3 mm diameter. In order to extract micro-sized beams from the PS discharge chamber, stainless steel collimating structures were attached to the anode. The hollow cathode cavity, also made of stainless steel, has a length of 50 mm and a diameter of 50 mm. An external energy storage capacitor C_{ext} of 600 pF across the cathode and anode was used to control the discharge duration and hence the electron beam duration. A rotary pump evacuated the experimental system from the anode end through a vacuum valve. The working gas (in this case, air) entered the chamber through a very fine adjustable needle valve at the anode side and its pressure was measured by a capacitance manometer-type vacuum gauge. The hollow cathode was connected through a charging resistor of 10 MΩ to a negative high voltage source while the anode was grounded. A capacitive voltage probe with a sub-nanosecond response time was connected to the cathode to measure the applied and discharge voltage. Measurements of the beam current were realized using a Rogowski current probe attached to the anode and followed by the drift tube.

When a high voltage is applied to the hollow cathode, the electric field across the anode-cathode gap penetrates a short distance into the hollow cathode region due to the small cathode aperture. A PS discharge will occur if the pressure in the system is suitably low (typically 50–500 mTorr and approximately 110 mTorr in this experiment) so that the discharge is at the left-hand side (with respect to the minimum) of the Paschen curve.[6] In such a PS discharge condition, the gas breakdown will occur along the longest possible path, allowing a virtual anode to form, extending from the anode into the hollow cathode region. As the virtual anode reaches, the cathode surface field-enhanced emission begins to occur. Electrons begin emitting from the cathode surface at an increased rate, augmented by secondary emission and

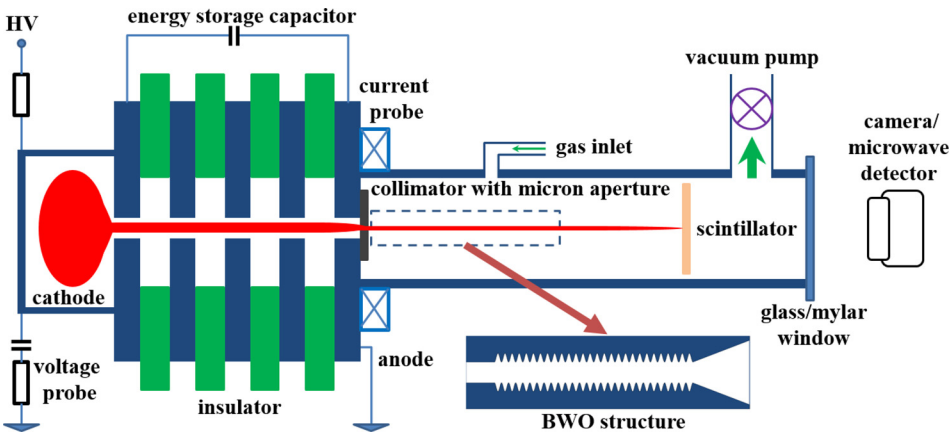

FIG. 1. Experimental setup of the micro electron beam generation from a pseudospark discharge and Backward Wave Oscillator (BWO) experiment.

are accelerated toward the aperture by the electric field. Consequentially, this rapid increase in electron emission results in a rapid increase in the beam current. As the beam propagates through the anode, its front edge ionizes the background gas, forming a plasma channel, while the following beam electrons expel part of the plasma electrons so that an ion-channel is formed, confining the beam and eliminating the need for any external magnetic guide field. A high current density, high brightness electron beam with a sweeping voltage can therefore be generated and propagated by ion channel focusing if the condition $1 - n_i/(n_b + n_{e0}) - \beta_b^2 \leq 0$ is satisfied,[12] where n_i, n_{e0} are the ion and trapped plasma electron density in the ion channel, respectively, and n_b is the beam electron density and β_b is the ratio of electron beam velocity to the speed of light.

The pulse duration of the pseudospark-based electron beam is adjustable by changing the parameters of the electric circuit powering the discharge.[13] Usually it is in the range of a few nanoseconds to a few hundred nanoseconds. In order to establish the viability of small-diameter PS-generated electron beams for BWO operation at THz frequencies, micro beams were investigated by using different collimators integrated within the anode of the PS device. Collimators with micro-aperture diameters of 1 mm, 500 μm, 200 μm, 100 μm, and 70 μm were attached to the PS anode, respectively, in order to extract micro beams of the corresponding sizes. Images of the generated beams were obtained by inserting a scintillator disk made from 1 μm thickness copper foil coated with scintillation powder (Plano P47, Agar Scientific Ltd., UK); 60 mm downstream of the anode with pictures taken with a high-speed digital camera is located at the end of the drift tube.

A 500 μm beam image was recorded and is shown in Fig. 2 when a collimator of 500 μm aperture size was used. Images of smaller beams were not recorded because the scintillator/camera combined sensitivity was not high enough, but beam current measurements of the smaller beams confirmed that the PS discharge was scalable to produce micro diameter (70 μm) beams for high frequency radiation applications. By using a second Rogowski probe, the electron beam was measured to propagate up to 20 cm downstream of the anode.[13] For the BWO interaction in the sub-terahertz range, a 1 mm diameter electron beam was used.

The SWS used as the BWO interaction region had a sinusoidal profile on its inner surface described by $r_w(\varphi, z) = r_0 + r_1 \sin(2\pi z/d)$, where r_0 is the mean radius, r_1 is the corrugation depth and d is the period. The operating modes for the beam-wave interaction are the transverse magnetic (TM) modes. In the SWS, the field can be expanded in a series of modes, in the form of $E_z = \sum_{n=-\infty}^{\infty} E_{zn}(r) \exp[i(k_n z - \omega t)]$, according to Floquet's theorem due to the periodic boundary condition. The electromagnetic field equations for the TM modes in cylindrical coordinates can therefore be obtained and the axial component of the electric field including the effect of the electron beam can be written as[14]

$$\frac{1}{r}\frac{d}{dr}\left(r\frac{dE_{zn}}{dr}\right) + \Gamma_n^2 E_{zn} = 0, \quad (r \neq r_b), \tag{1}$$

where $\Gamma_n^2 = (\omega/c)^2 - k_n^2$ and $k_n = k_z + 2\pi n/d$, here $k_z \in [-\pi/d, \pi/d]$. It has the solution

$$E_{zn} = \begin{cases} A_n J_0(\Gamma_n r), & 0 \leq r \leq r_b \\ B_n J_0(\Gamma_n r) + C_n N_0(\Gamma_n r), & r_b < r \leq r_w \end{cases}. \tag{2}$$

Applying the boundary condition of the tangential electric field $E_{w\perp} = 0$ at the waveguide wall and the continuity of E_{zn} at r_b which is the beam radius, B_n and C_n can be written in terms of A_n and finally a homogeneous matrix equation of $D_n \cdot A_n = 0$ can be derived where D_n is a matrix of the unknown parameters ω, k_z. The dispersion relations can be determined by solving the equation $\det[D_n] = 0$. The operating mode in the BWO is the lowest TM_{01} mode which has the strongest beam-wave coupling. The radiation wave will

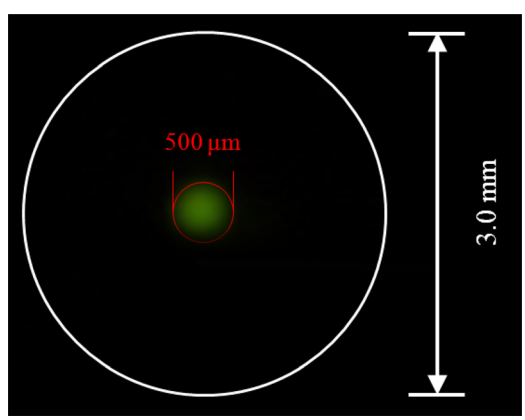

FIG. 2. Image of electron beam imprint on phosphor scintillator for a single pulse. The electron beam diameter represented by the central bright spot was measured to be 500 μm.

be excited when the Doppler shift term for the plasma oscillation in the beam, $k_z v_z$, is close to the dispersion relation of the SWS ensuring extended phase synchronism.

For the PS-based BWO experiment, a plasma background forms in the SWS due to the ionization of the neutral background gas. After consideration of the beam plasma frequency $\omega_{be} = (e^2 n_b/\gamma\varepsilon_0 m_e)^{1/2}$ and the Doppler shift term, the beam dispersion becomes $\omega = k_z v_z \pm \omega_{be}$, where γ is the relativistic factor of the electron beam and m_e is the electron rest mass. The plasma loading will also affect the dispersion characteristic of the waveguide with, or without, a magnetic field.[15] If the plasma background is uniformly distributed inside the waveguide, then the equivalent relative dielectric constant can be written as $\varepsilon = 1 - (\omega_{pe}/\omega)^2$, where $\omega_{pe} = (e^2 n_e/\varepsilon_0 m_e)^{1/2}$ is the plasma oscillation frequency and n_e is the electron density in the plasma. This gives a correction factor of ε to the Γ_n^2 in the electromagnetic field equations. Using the same method as for the case without plasma loading, the dispersion curve $\omega(k_z)$ can be numerically solved but with a more complicated form.[16,17] The calculated results show that the dispersion curve can be significantly upshifted if the plasma density is high enough.

The experimental measurement of the pseudospark discharge gives a plasma density in the order of 10^{19} to $10^{20}\,\mathrm{m}^{-3}$, which was confirmed by the 2D Particle-In-Cell (PiC) simulation of the electron beam transportation in a plasma background using MAGIC.[18,19] Stable propagation of the electron beam, which happens during the pseudospark discharge process, requires a plasma density of approximately $6.5 \times 10^{19}\,\mathrm{m}^{-3}$ under the discharge conditions of the experiment. The electron beam will not propagate stably in a higher plasma density and becomes defocused in a lower value.

Fig. 3 shows the dispersion relations of the TM_{01} mode in a smooth vacuum waveguide (transposed by the space harmonic, $2\pi/d$) and the TM_{01} eigenmode in the BWO SWS under different plasma densities. The dimensions used in the simulations are the same as those used in the experiments, namely, $r_0 = 610\,\mu$m, $r_1 = 130\,\mu$m, and $d = 470\,\mu$m with a beam wave interaction length of 25 periods. The slow wave

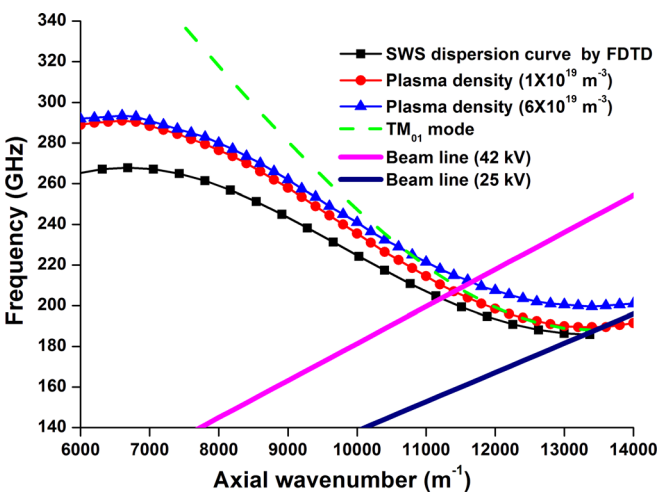

FIG. 3. Dispersion relations of the TM_{01} eigenmode in the BWO structure under different plasma densities and Doppler-upshifted plasma wave mode from electron beam.

structure was designed to be able to interact over a large beam voltage range to maximize the output power and frequency range. The length of the SWS was optimized from the numerical simulation of the beam-wave interaction using PIC code MAGIC. In the simulation the variation of the beam voltage and current with time was taken into account according to their measured waveforms.

The dispersion curve of the operating TM_{01} eigenmode without electron beam and plasma was verified using the 3D finite-difference time-domain code CST Microwave Studio. The intersection between the dispersion curve and the electron beam line is the approximate radiation frequency. The Doppler shifted dispersion lines for electron beam energies of 42 keV and 25 keV are also plotted in Fig. 3.

The BWO structure (Fig. 4), together with the conical radiation launching horn, was manufactured by high speed grinding of an aluminum former and the subsequent electrodeposition of a 5 mm thick layer of copper on the aluminum former, which was later dissolved away in an alkali solution.

The PS discharge was initiated with a collimator of aperture size 1 mm and the rippled-wall BWO SWS was integrated into the anode aperture. The SWS position is indicated by the dashed rectangular box in Fig. 1. Radiation pulses were measured using a semiconductor rectifying diode (ELVA-1 Microwave Ltd., ZBD-05, 140–220 GHz) situated 30 mm from the BWO launching horn. A heterodyne frequency diagnostic was used to measure the frequency of the output radiation of the BWO. A sub-harmonic mixer (Millitech MSH-05-2NI00) and a local oscillator signal produced from a 95 GHz Gunn diode (Millitech GDM-10-1013IR) were used and the resultant intermediate frequency (IF) signal was recorded using a 20 GHz, deep memory digitizing oscilloscope (Agilent DSX-X 92004 A).

Fig. 5 shows the repeatable time-correlated electron beam voltage, the discharge current and the millimeter wave pulse. The electron beam current has a step of about 5 A at the hollow cathode discharge phase and then a peak current of about 10 A follows in the conductive phase. The microwave radiation was mainly generated near this first 5 A step, because the correlated beam voltage has stronger coupling with the BWO structure. In the conductive phase, the beam voltage is too small to have efficient beam-wave interaction.

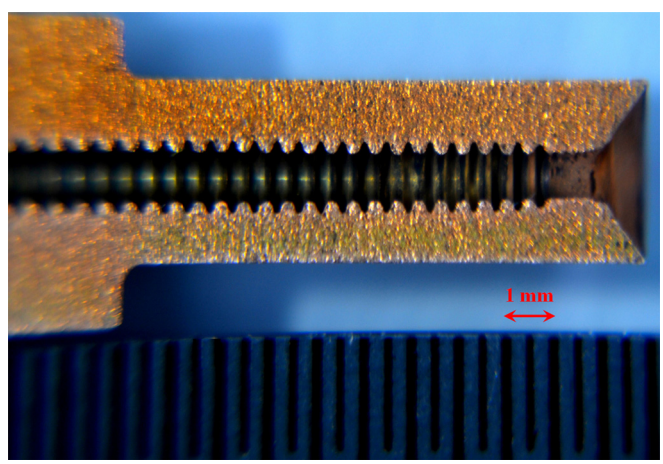

FIG. 4. A photograph of the BWO structure.

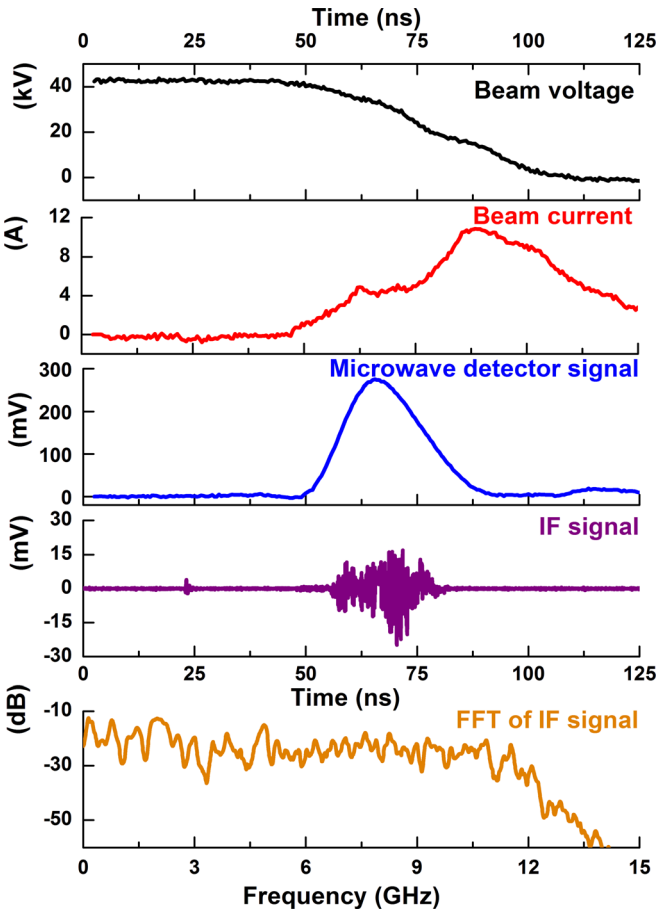

FIG. 5. Time-correlated electron beam voltage, current pulse, the radiation pulse from the 200 GHz BWO, the IF output from a harmonic mixer recorded on a deep memory (20 GHz) single shot digital storage oscilloscope, and FFT result of the intermediate frequency output.

The output power was ascertained using the general antenna theorem with the total power from a launching antenna, calculated by integrating its radiated power density over space. The integration was completed by numerically integrating the normalized mode profile of the launching horn and multiplying by the measured maximum power density. In doing so, the total power of the BWO in this frequency range was found to be 20 W.

By applying a fast Fourier transform (FFT) to the IF signal recorded by the fast digitizing oscilloscope, it was then possible to determine the frequency spread of the emitted pulse, which may be seen in Fig. 5. The FFT of the IF signal indicates a frequency spread of 12 GHz. As the subharmonic mixer operates at the second harmonic of the local oscillator frequency at 95 GHz and the cut-off frequency of the operating mode in the SWS was 186 GHz, the measured frequency band of the BWO was determined to be 186–202 GHz.

This paper demonstrates the potential to combine handheld terahertz sources and high-power sources into one device. In addition, the generation of smaller electron beams from the PS source show the potential for the generation of signals moving towards the mid-THz range while still producing powers which rival, if not exceed, those of vacuum electronic sources operating at similar frequencies. As such, while these experimental results are a major advance and have matched well with the output predicted by simulations, they may be seen as an indicator of even greater performance in the future, making such PS-plasma assisted BWO devices of great interest in a variety of application areas.

The authors would like to thank the Engineering and Physical Sciences Research Council (EPSRC) for supporting this work, under Research Grant EP/G011087/1 and EP/K029746/1.

[1]M. Mineo and C. Paoloni, Prog. Electromagn. Res. Lett. **30**, 163 (2012).
[2]R. M. G. M. Trines, F. Fiuza, R. Bingham, R. A. Fonseca, L. O. Silva, R. A. Cairns, and P. A. Norreys, Nat. Phys. **7**, 87 (2011).
[3]K. R. Chu, Rev. Mod. Phys. **76**, 489 (2004).
[4]W. He, C. R. Donaldson, L. Zhang, K. Ronald, P. McElhinney, and A. W. Cross, Phys. Rev. Lett. **110**, 165101 (2013).
[5]H. Yin, A. Cross, W. He, A. Phelps, and K. Ronald, IEEE Trans. Plasma Sci. **32**, 233 (2004).
[6]K. Frank and J. Christiansen, IEEE Trans. Plasma Sci. **17**, 748 (1989).
[7]A. Sengupta, in *Proceedings of 29th International Electric Propulsion Conference* (2005), pp. 1–17, Paper No. IEPC-2005-026.
[8]J. Christiansen and C. Schultheiss, Z. Phys. A **290**, 35 (1979).
[9]H. Yin, A. W. Cross, W. He, A. D. R. Phelps, K. Ronald, D. Bowes, and C. W. Robertson, Phys. Plasmas **16**, 063105 (2009).
[10]A. W. Cross, H. Yin, W. He, K. Ronald, A. D. R. Phelps, and L. C. Pitchford, J. Phys. D: Appl. Phys. **40**, 1953 (2007).
[11]E. Dewald, K. Frank, D. Hoffmann, M. Ganciu, N. Mandache, M. Nistor, A. Pointu, and I.-I. Popescu, Nucl. Instrum. Methods Phys. Res., Sect. A **415**, 614 (1998).
[12]S. B. Swanekamp, J. P. Holloway, T. Kammash, and R. M. Gilgenbach, Phys. Fluids B **4**, 1332 (1992).
[13]H. Yin, W. He, A. W. Cross, A. D. R. Phelps, and K. Ronald, J. Appl. Phys. **90**, 3212 (2001).
[14]J. A. Swegle, J. W. Poukey, and G. T. Leifeste, Phys. Fluids **28**, 2882 (1985).
[15]L. Shenggang, Y. Yang, M. Jie, and D. M. Manos, Phys. Rev. E **65**, 036411 (2002).
[16]M. M. Ali, K. Minami, K. Ogura, T. Hosokawa, H. Kazama, T. Ozawa, T. Watanabe, Y. Carmel, V. L. Granatstein, W. W. Destler, R. A. Kehs, W. R. Lou, and D. Abe, Phys. Rev. Lett. **65**, 855 (1990).
[17]M. Botton, Appl. Phys. Lett. **60**, 2198 (1992).
[18]T. Kamada, T. Fujiwara, M. Itagaki, T. Ishikawa, and M. Watanabe, Jpn. J. Appl. Phys., Part 1 **44**, 6747 (2005).
[19]T. Gray, D. N. Smithe, and L. D. Ludeking, *Introduction to MAGIC* (Mission Research, Newington, VA, 2003).